

# Accepted Manuscript

The synthesis of  $\text{Cu}_x\text{S}$  from Cu layers by low pressure plasma processing

J. Ball, D.W. Lane, H.S. Reehal

PII: S0925-8388(17)30780-6

DOI: [10.1016/j.jallcom.2017.03.011](https://doi.org/10.1016/j.jallcom.2017.03.011)

Reference: JALCOM 41049

To appear in: *Journal of Alloys and Compounds*

Received Date: 24 November 2016

Revised Date: 20 February 2017

Accepted Date: 2 March 2017

Please cite this article as: J. Ball, D.W. Lane, H.S. Reehal, The synthesis of  $\text{Cu}_x\text{S}$  from Cu layers by low pressure plasma processing, *Journal of Alloys and Compounds* (2017), doi: 10.1016/j.jallcom.2017.03.011.

This is a PDF file of an unedited manuscript that has been accepted for publication. As a service to our customers we are providing this early version of the manuscript. The manuscript will undergo copyediting, typesetting, and review of the resulting proof before it is published in its final form. Please note that during the production process errors may be discovered which could affect the content, and all legal disclaimers that apply to the journal pertain.



# The synthesis of $\text{Cu}_x\text{S}$ from Cu layers by low pressure plasma processing

J Ball<sup>a\*</sup>, D W Lane<sup>b</sup> & H S Reehal<sup>a</sup>

<sup>a</sup>School of Engineering, London South Bank University, 103 Borough Road, London SE1 0AA, UK.

<sup>b</sup>Materials Science and Radiation Group, Cranfield Forensic Institute, Cranfield, Defence and Security, Cranfield University, Shrivenham, Swindon, SN6 8LA, UK

\*Corresponding author

## Abstract:

A new method of converting Cu layers to  $\text{Cu}_x\text{S}$  on glass at low pressure using an electron cyclotron resonance plasma and  $\text{SF}_6$  gas is presented. The process operates at low temperatures and short time scales. Trends in film crystallinity and morphology are identified in relation to process time and temperature. These show that sulphurisation is most likely complete within 10 minutes and that the sulphur content of the films reduces as the conversion temperature is increased from 473 to 623 K. Optical measurements show that the films have a direct bandgap of  $\sim 2.5$  eV which is consistent with published values for  $\text{Cu}_x\text{S}$  films grown by other techniques. Analysis by SEM has revealed that the films possess a complicated structure of platelets covering a denser underlying film. This may account for the differences in observations made by XRF and Raman spectroscopy, which both indicated a mixture of CuS and  $\text{Cu}_2\text{S}$ , and X-ray diffraction which predominantly showed CuS.

**Key words:** semiconductors, thin films, vapour deposition, SEM, X-ray diffraction,

## 1 Introduction:

Copper sulphide ( $\text{Cu}_x\text{S}$ ) in its various phases (Covellite ( $\text{CuS}$ ), anilite ( $\text{Cu}_{1.75}\text{S}$ ), digenite ( $\text{Cu}_{1.8}\text{S}$ ), djurleite ( $\text{Cu}_{1.95}\text{S}$ ), and chalcocite ( $\text{Cu}_2\text{S}$ )), has many potential applications in optical and electronic devices. These include transparent conductive contacts [1], coatings for microwave shielding [2], biosensors [3] and solar cells [4]. Synthesis of  $\text{Cu}_x\text{S}$  has been achieved with a number of techniques including the liquid–liquid interface reaction [5], metal organic and aerosol assisted chemical vapour deposition (MOCVD and AACVD) [6], chemical vapour reaction (CVR) [7] and atomic layer deposition (ALD) [8]. Chemical bath deposition (CBD) has also been used with applications for dye sensitised solar cells [9] and in nanowisker form [10].

Synthesis of  $\text{Cu}_x\text{S}$  by MOCVD typically takes place at 723 K to 773 K for 60 minutes while AACVD demonstrated deposition at the same temperatures for process times between 30 and 60 minutes [6]. Direct reactions between copper and sulphur have demonstrated formation of copper sulphides [11] but it has been suggested that for reactions below 423 K material

conversion is restricted to the surface [12]. Overcoming this drawback has required the use of high temperature [11], or solvents [13].

CBD techniques while operating at temperatures  $<363$  K require deposition times from 1 to 12 hours [14,15] where films fabricated in an hour were non-uniform and poor in quality. Bagul et.al. [16] reported a solution based method with deposition temperatures optimised at 343 K and growth taking place for 3.5 hours.

Films have also been fabricated via the spray pyrolysis technique [17] with substrate temperature varying between 458 K to 558 K. The spraying sequences varied between 15 and 40 minutes [17] depending on precursor solution. Variations in the CuS films surface morphology featured crystal sizes dependant on the different precursor solutions and sample temperatures. Using this technique Gadgil et.al. [18] reported  $\text{Cu}_2\text{S}$  chalcocite as the dominant phase in films deposited at 523 K.

Reactively sputtered  $\text{Cu}_x\text{S}$  deposition has been carried out at temperatures ranging from ambient to 773 K. Typically Cu targets are sputtered in an argon plasma with the addition of  $\text{H}_2\text{S}$  [19]. Copper coexists in the film if the  $\text{H}_2\text{S}$  flow is too low, while with increasing gas flow and decreasing sputter power, CuS films with hexagonal structure can be fabricated.

Other plasma techniques have also been employed to produce  $\text{Cu}_x\text{S}$ . Randhawa et.al. [20] used activated reactive evaporation (ARE). This process involves the resistive evaporation of Cu in a  $\text{H}_2\text{S}$  plasma with substrate temperatures ranging from 298 K to 593 K producing chalcocite ( $\text{Cu}_2\text{S}$ ). Varying process conditions yielded changes in the materials resistivity and surface morphology.

In this paper we present the first results for the synthesis of  $\text{Cu}_x\text{S}$  from thin Cu layers on glass substrates by electron cyclotron resonance (ECR) plasma excitation. ECR chemical vapour deposition (ECRCVD) is a plasma enhanced process where a precursor gas is ionised by a 2.45 GHz microwave source and induced into a resonant condition by the use of an electromagnet [21]. Typically, this technique has been used for thin film Si deposition [22], etching [23] and nanowire growth [24]. We demonstrate that this technique has the potential to convert Cu to  $\text{Cu}_x\text{S}$  at low temperatures and short process times using  $\text{SF}_6$  as the source of sulphur.

## 2 Material and methods:

Corning glass samples were cleaned in acetone in an ultra-sonic bath followed by a deionised water rinse and  $\text{N}_2$  blow dry. This was followed by a 3:1  $\text{H}_2\text{SO}_4$ : $\text{H}_2\text{O}_2$  etch for 10 minutes, DI rinse and final  $\text{N}_2$  blow dry prior to loading into a KJL PVD 75 ebeam system. After pumping to a base pressure of  $\sim 5 \times 10^{-5}$  Pa,  $\sim 150$  nm of 4N Cu was deposited onto the samples with the thickness determined during deposition by a crystal thickness monitor. The thicknesses of the as-deposited layers were confirmed post deposition with a Dektak 6M stylus profilometer.

The glass/Cu samples were loaded into the ECRCVD system and the heater was ramped to the required process temperature in vacuum to allow outgassing and temperature stabilisation.

At this point SF<sub>6</sub> was introduced into the chamber and plasma processing commenced. Processing parameters are given in table 1.

Table 1: plasma processing parameters

Parameter	Value
MW power (W)	800
Magnet Current (A)	5
Process time (min)	10, 30, 60
SF <sub>6</sub> flow rate (m <sup>3</sup> /s)	3.33x10 <sup>-7</sup>
Process pressure (Pa)	1.33
Temperature (K)	373, 473, 523, 573, 623, 673

Upon completion of the process time the heater was turned off and samples were left to cool under vacuum. Subsequently the samples were analysed using a Renishaw Raman system using the 488 nm line of an Ar<sup>+</sup> ion laser with a spatial resolution of ~1µm. Surface morphology was characterised with a Hitachi S4300 scanning electron microscope (SEM). Optical characterisation of the sample reflection and transmission was carried out using a Bentham PVE 300 system.

The composition of the sulphurised films was determined by X-ray fluorescence (XRF) using a SII NanoTechnology Inc. SEA6000VX spectrometer operating at 15 kV. Spectra were analysed using the instrument's film fundamental parameters software which was calibrated using XRF thin film reference standards for Cu and Cu<sub>x</sub>S (MICROMATTER Technologies Inc., Canada). These were placed directly on top of a blank substrate to more accurately represent the structure of the samples. Crystallographic phase determination was done by X-ray diffraction (XRD) using a Philips Panalytical X'Pert Pro diffractometer operating with  $\theta/\theta$  geometry, Cu K $\alpha$ 1 radiation (wavelength 0.154 nm), and using the ICDD powder diffraction database [25]. The analysed areas of the samples were 1.2 mm  $\times$  1.2 mm during XRF and 10 mm diameter during XRD when the samples were rotated during data collection.

### 3 Results:

Samples processed below 473 K and at 673 K delaminated upon removal from the ECRCVD system with no further analysis possible. Control samples of the same Cu thickness were processed at the same temperatures, SF<sub>6</sub> flow rates, pressures and times but without a plasma. These control samples exhibited no evidence of material conversion.

The variation in the chemical composition of the sulphurised films as determined by XRF is presented in figure 1. This shows that the sulphur content of the films reduced as the process temperature increased, with a stoichiometry that is broadly consistent with CuS at low temperatures and Cu<sub>2</sub>S at high temperatures. At 573 K little variation in sulphur content was observed for processing times between 10 and 60 minutes.

Figure 1a & 1b

Figure 1: XRF analysis of sulphur content  $x$  ( $\text{CuS}_x$ ) for samples after processing. (a) The effect of growth temperature for 60 minute deposition runs, apart from the 623 K run which was for 30 minutes. (b) The effect of deposition time for 573 K deposition temperature.

Figures 2 and 3 show the results of the XRD analysis, which revealed the presence of several sulphide phases without any indication of metallic Cu. The films processed at 573 K (figure 2) were predominantly covellite ( $\text{CuS}$ ). Little variation in the crystallographic structure with increasing process times from 10 to 60 minutes was observed, apart from the appearance of the (008) reflection after processing for 30 minutes.

Figure 2

Figure 2 XRD analysis for samples grown at 573 K for different process times. Labelled reflections are for covellite  $\text{CuS}$  (ICDD 79-2321).

The effect of changing the process temperature was also examined by XRD and the results are shown in figure 3.

Figure 3

Figure 3 XRD analysis of samples grown at different temperatures. Growth time 60 minutes apart from 623 K which was for 30 minutes. Labelled reflections are for covellite  $\text{CuS}$  (ICDD 79-2321), \*digenite  $\text{Cu}_{1.8}\text{S}$  (ICDD 47-1748) and \*\*chalcocite  $\text{Cu}_{1.96}\text{S}$  (ICDD 29-578).

At 473 K the film can be seen to be quite poorly crystalline with broad reflections that were again consistent with covellite. As the temperature increased up to 573 K the films remained covellite and their diffraction peaks became sharper as their crystallinity increased. At 623 K the crystallographic phase changed to a mixture of digenite ( $\text{Cu}_{1.8}\text{S}$ ) and possibly nonstoichiometric chalcocite ( $\text{Cu}_{1.96}\text{S}$ ), the peak at approximately  $33^\circ$  being the strongest reflection reported for this phase (103) in the ICDD powder diffraction data file (29-578). These phases have been observed by Nair et al [26] for the conversion of chemically deposited  $\text{CuS}$  thin films by annealing at 673 K under nitrogen.

The XRD data was used to determine the degree of preferred orientation within the films by comparing the intensities of the observed Bragg reflections to those given by the ICDD powder diffraction data file (79-2321) using equation 1.

$$C_{hkl} = \frac{\frac{I_{hkl}}{I_{hkl}^R}}{\frac{1}{n} \sum \frac{I_{hkl}}{I_{hkl}^R}} \quad (1)$$

Here  $C_{hkl}$  is the texture coefficient for the (hkl) reflection,  $I_{hkl}$  is the observed intensity for the reflection and  $I_{hkl}^R$  is the corresponding listed intensity from the ICDD powder diffraction data.  $n$  is the number of reflections included in the analysis. The resulting texture coefficients for the covellite films are summarised in table 2.

Table 2: The texture coefficient observed for the covellite films.

hkl	Texture coefficient, $C_{hkl}$					
	Annealing time (at 573K)			Annealing temperature (for 60 min, 623 K 30 min)		
	10 min	30 min	60 min	473 K	523 K	623 K
102	$97 \times 10^{-2}$	$71 \times 10^{-2}$	$71 \times 10^{-2}$	$133 \times 10^{-2}$	$23 \times 10^{-2}$	$71 \times 10^{-2}$
103	$81 \times 10^{-2}$	$50 \times 10^{-2}$	$52 \times 10^{-2}$	$49 \times 10^{-2}$	$16 \times 10^{-2}$	$52 \times 10^{-2}$
006	$185 \times 10^{-2}$	$367 \times 10^{-2}$	$343 \times 10^{-2}$	$140 \times 10^{-2}$	$554 \times 10^{-2}$	$343 \times 10^{-2}$
110	$84 \times 10^{-2}$	$35 \times 10^{-2}$	$39 \times 10^{-2}$	$135 \times 10^{-2}$	$3 \times 10^{-2}$	$39 \times 10^{-2}$
108	$94 \times 10^{-2}$	$60 \times 10^{-2}$	$67 \times 10^{-2}$	$116 \times 10^{-2}$	$2 \times 10^{-2}$	$67 \times 10^{-2}$
116	$58 \times 10^{-2}$	$17 \times 10^{-2}$	$28 \times 10^{-2}$	$28 \times 10^{-2}$	$1 \times 10^{-2}$	$28 \times 10^{-2}$

These show that the majority of the films are dominated by the (006) reflection, which appears to reach a maximum at an annealing temperature of 523 K.

The Raman spectroscopy results taken at multiple points on the samples generally indicate an inhomogeneous conversion of the initial Cu layers. The results shown in figure 4 are representative of the measured spectra (presented in supplementary data) and include reference spectra from several  $\text{Cu}_x\text{S}$  phases.

The Raman spectra samples processed for 10, 30 and 60 minutes at 573 K are shown in figure 4(a). The spectra for 30 and 60 minutes indicate mixed  $\text{Cu}_2\text{S}/\text{CuS}$ , while the 10 minute sample suggests a dominant presence of  $\text{Cu}_2\text{S}$ .

Figure 4 a b c

Figure 4 (a) Raman spectra for 10, 30 and 60 minutes at 573 K process (b) Raman spectra for 60 minutes process at 473 K, 523 K, 573 K and 623 K (c) Raman spectra of sample processed for 30 min at 623 K.

The effect of changing process temperature can be seen in figure 4(b) where the 473 K process for 60 minutes suggests a possible mixed  $\text{Cu}_2\text{S}/\text{CuS}$  film of poor quality. Films processed at 523 K and 573 K suggest a mixture of  $\text{CuS}$  and  $\text{Cu}_2\text{S}$ . The 30 minute run at 623 K has a highly defined  $\text{CuS}$  peak with possible additions of  $\text{Cu}_{1.96}\text{S}$  and  $\text{Cu}_{1.8}\text{S}$  as seen from figure 4(c).

The optical transmission of the samples over a range of 300-1100 nm can be seen in figure 5, with samples processed at 573 K for 10, 30 and 60 minutes shown in figure 5(a). A transmission peak can be seen in the region of  $\sim 550$  nm which attenuates with decreasing time.

Figure 5 a and b

Figure 5: Transmission of samples (a) 573 K process for 60, 30 and 10 minutes (b) 573 K, 523 K and 473 K processes for 60 minutes and 623 K process for 30 minutes.

A similar but more pronounced trend can be seen with the change in process temperature in figure 5(b). Decreasing temperature from 573 K to 473 K decreases transmission with a broadening and shift to the longer wavelengths at the lowest temperature. Processing for 30 minutes at 623 K gives the highest level of transmission.

The reflection of the films is presented in figure 6. Samples processed at 573 K decreasing in process time from 60 to 10 minutes show a reduction in reflection from a peak at ~800 nm broadening significantly at 10 minutes (figure 6(a)).

Figure 6 a and b

Figure 6: Reflection of samples (a) 573 K processed for 60, 30 and 10 minutes (b) 573 K, 523 K and 473 K processed for 60 minutes and 623 K processed for 30 minutes.

Decreasing process temperatures from 573 K to 523 K and then 473 K (figure 6(b)) demonstrates a significant drop in reflection at wavelengths >700nm. Interestingly, increasing process temperature to 623 K for a shorter 30 minute run typically shows a decrease in reflection at wavelengths >700 nm but an increase <700 nm.

The optical band gaps of the allowed direct transitions were obtained from Tauc plots (shown in figure 7) of  $(\alpha h\nu)^2$  against  $h\nu$ . Here  $h$  is Plank's constant,  $\nu$  frequency and  $\alpha$  absorption coefficient. Transmission was corrected and absorption coefficient calculated following the method of Nair et.al. [26].

Figure 7 a and b

Figure 7: Plots of  $(\alpha h\nu)^2$  against  $h\nu$  for (a) films processed for 10, 30 and 60 minutes at 573 K, (b) films processed at 473 K, 523 K, 573 K for 60 minutes and 623 K for 30 minutes.

Figure 7(a) shows the optical band gap for the samples processed at 573 K for 10, 30 and 60 minutes. It can be seen that with increasing process time the band gap decreases, varying from ~2.56 eV to ~2.54 eV and ~2.51 eV for processing times of 10, 30 and 60 minutes, respectively. The films processed at increasing temperatures for 60 minutes, as shown in figure 7(b), show a band gap of ~ 2.51 eV for samples processed at 473 K, 523 K and 573 K. The sample processed at 623 K for 30 minutes had a band gap of ~2.62 eV. These are in a similar range to those reported for direct transitions in  $\text{Cu}_2\text{S}$  films grown from solution [17, 27,].

SEM analysis showing the morphological variations of the sample surface can be seen in figure 8.

Figure 8

Figure 8: SEM micrographs for films processed for (A) 60 minute at 473 K (B) 60 minute at 523 K (C) 60 minute at 573 K (D) 30 minute at 573 K (E) 10 minutes at 573 K (F) 30 minutes at 623 K (scale bar 10  $\mu\text{m}$  and applicable to all samples).

It can be seen when comparing images A, B and C that increasing process temperature with a 60 minute run time changes surface features. At 473 K (figure 8 A) the surface included small needle like structures embedded in small grains. Increasing temperature introduces a change to polygonal like structures at 523 K (figure 8 B). At 573 K (figure 8 C) these maintain their morphology but increase in size with reduced density.

Decreasing process time at 573 K from 60 minute to 30 minute to 10 minutes (figures 8 C, D and E respectively) generates smaller but denser features. Increasing the process temperature to 623 K for 30 minutes (figure 8 F) generates a different surface finish with no polygonal structures at this level of magnification. Instead we see the formation of what are possibly small grains.

#### 4 Discussion:

The XRF results in figure 1 and XRD results in figures 2 and 3 indicate that the sulphurisation process converting the initial Cu layers to  $\text{Cu}_x\text{S}$  has been successful.

The variation in the chemical composition of the sulphurised films as determined by XRF in figure 1 shows that the sulphur content of the films reduced as the process temperature increased, with a stoichiometry that is broadly consistent with  $\text{CuS}$  at low temperatures and  $\text{Cu}_2\text{S}$  at high temperatures. We suggest reduction in the film's sulphur content with increasing temperature is the result of desorption due to the low melting point of sulphur at 388 K [16].

At 573 K little variation in sulphur content was observed for annealing times between 10 minutes and 60 minutes, which indicates that conversion to the sulphide occurs quite rapidly during the process and that the observed compositions can be considered to be at chemical equilibrium.

The effect of changing the annealing temperature is also examined by the XRD results of figure 3. The changes observed were similar to those for the chemical composition of the films in that the effects of changing the annealing temperature were far more dramatic than those for changing the annealing time.

The crystal orientation information in table 2 shows the majority of the films are dominated by the (006) preferred orientation, which appears to reach a maximum at an annealing temperature of 523 K.

For the series of samples processed with increasing temperature, the Raman data indicates that the conversion was not homogeneous with some results contradicting the XRF and XRD data. At low temperatures XRF data suggests a dominant  $\text{CuS}$  phase changing to  $\text{Cu}_2\text{S}$  with increasing temperature. The Raman results differ, showing mixed phases with an increase in  $\text{CuS}$  at 573 K. The XRF data is more in agreement with the XRD results with the exception of the 573 K film processed for 60 minutes.

When process time is varied from 10 minutes to 60 minutes, the covellite identified by the XRD is typically seen as chalcocite by XRF analysis, with the Raman results indicating a mixed phase.

The morphology of the samples exhibit change as can be seen from the SEM images in figure 8 A-C. A clear trend can be seen where increasing process temperature results in changing surface features, from small needles to small polygons to large polygons. Increasing process time at a set 573 K (images C, D and E) shows an increase in surface feature size. Image F suggests small  $\text{Cu}_x\text{S}$  grains were formed in the film processed at 623 K as observed by Wang et. al. [7].

The discrepancy observed between the results at certain points in the sample space could be attributed to this varied surface morphology. Raman spectroscopy with its small probe size ( $\sim 1\mu\text{m}$  diameter) relative to XRD ( $\sim 10\text{ mm}$  diameter and rotated) and XRF ( $\sim 1.2\text{ mm} \times 1.2\text{ mm}$ ) indicates the conversion from Cu is probably inhomogeneous for these process conditions resulting in multiple phases; an observation we suspect to be correct given the fabrication of mixed phase films by Ren et.al. [28]. It is possible that the results obtained from XRD and XRF are dominated by different sample features which gives rise to the contradictory results. Other groups have reported surface features similar to those observed in images C, D and E in figure 8. The  $\text{Cu}_{1.96}\text{S}$  platelets of Kemmler et. al. [6] were grown on a glass substrate using low pressure MOCVD at 723 K for 60 minutes. CBD on FTO coated glass slides carried out by Xin et.al. [29] demonstrated such structures were CuS. Wang et.al.[30] grew single-crystalline CuS plates via chemical vapour reaction reacting Cu films on glass substrates in a vacuum chamber with sulphur vapour at  $\sim 723\text{ K}$  for  $\sim 7$  hours. Following Wang et.al. [30] we suggest the platelets observed in figure 8 C, D and E are probably CuS growing in an underlying  $\text{Cu}_x\text{S}$  matrix. The discrepancy between XRD and XRF could be due to the domination of the XRD results by these CuS platelets over the less crystalline underlying layer.

The trends in the optical data show an increase in transmission and reflection with increasing process time at 573 K. A similar trend can be seen in the transmission of samples processed from 473 K through 523 K to 573 K with the transmission of the sample processed at 623 K showing a significant increase. This suggests that the surface morphology and material type, especially in the sample identified as digenite/chalcocite, is having an effect on the optical properties of the films. This change in transmission between digenite/djurleite and covellite has also been observed by Nair et.al. [15] supporting the XRD results for this sample.

Direct gaps varying between 2.36 and 2.4 eV have been observed for  $\text{Cu}_x\text{S}$  polycrystalline films [27, 31]. The band gaps derived from the Tauc plots in this work agree broadly with the literature given the inaccuracies associated with this method.

## 5 Conclusion:

We have demonstrated the complete conversion of Cu thin films on glass to  $\text{Cu}_x\text{S}$  using an ECR plasma excitation source and  $\text{SF}_6$  as the process gas. Samples were converted at temperatures ranging from 473 K to 623 K with a process time varying from 10 to 60 minutes

and demonstrate increasing CuS crystallinity with process temperature and time. From SEM images we have observed changes in film morphology corresponding with changes in process time and temperature. Increasing process temperature reduces the levels of S incorporation within the film.

Further work is being carried out to ascertain the limits of this versatile conversion method and its potential to other sulphide materials. Of particular interest are alloys such as CZTS which are attracting considerable interest as earth abundant materials for solar cells [32, 33, 34].

Acknowledgements:

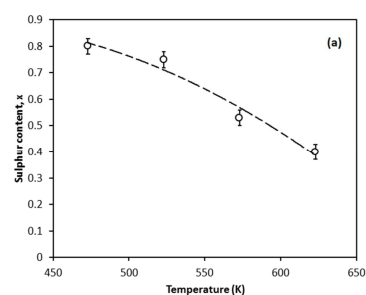
We thank London South Bank University for support.

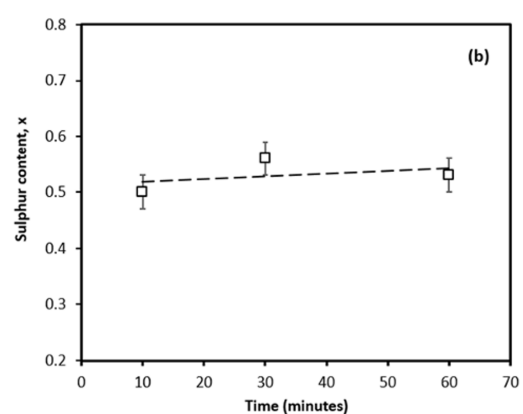
## References

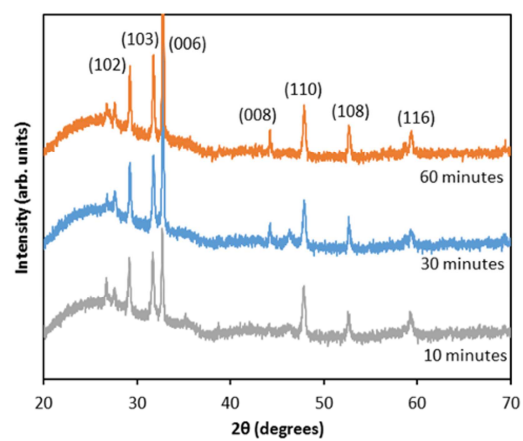
- [1] I. Grozdanov, M. Najdoski, Optical and Electrical Properties of Copper Sulfide Films of Variable Composition, *J. Solid State Chem.*, 114, (1995), 469–475.
- [2] I. Grozdanov, Deposition of electrically conductive, microwave shielding and IR-detecting inorganic coatings on polymer films, *Chem. Lett.*, 23, (1994), 551-554.
- [3] H. Lee, S.W. Yoon, E.J. Kim, J. Park, In-situ growth of copper sulfide nanocrystals on multiwalled carbon nanotubes and their application as novel solar cell and amperometric glucose sensor materials, *Nano Lett.*, 7, (2007), 778–784.
- [4] D. B. Mitzi, O. Gunawan, T. K. Todorov, K. Wang, S. Guha, The path towards a high-performance solution-processed kesterite solar cell, *Sol. Energy Mater. & Sol. Cells*, 95, (2011), 1421–1436.
- [5] C.N.R. Rao, K.P. Kalyanikutty, The Liquid–Liquid Interface as a Medium To Generate Nanocrystalline Films of Inorganic Materials, *Acc. Chem. Res.*, 41, (2007), 489–499.
- [6] M. Kemmler, M. Lazell, P.O. Brien, D.J. Otway, J.-H. Park, J.R. Walsh, The growth of thin films of copper chalcogenide films by MOCVD and AACVD using novel single-molecule precursors, *J. Mater. Sci.: Mater. Electron.*, 13, (2002), 531–535.
- [7] K.J. Wang, G.D. Li, J.X. Li, Q. Wang, J.S. Chen, Formation of Single-Crystalline CuS Nanoplates Vertically Standing on Flat Substrate, *Cryst. Growth Des.*, 7, (2007), 2265–2267.
- [8] J. Johansson, J. Kostamo, M. Karppinen, L. Niinistö, Growth of conductive copper sulfide thin films by atomic layer deposition, *J. Mater. Chem.*, 12, (2002), 1022–1026.
- [9] K.D. Yuan, J.J. Wu, M.L. Liu, L.L. Zhang, F.F. Xu, L.D. Chen, F.Q. Huang, Fabrication and microstructure of pp-type transparent conducting CuS thin film and its application in dye-sensitized solar cell, *Appl. Phys. Lett.*, 93, (2008), 132106.
- [10] I. Puspitasari, T.P. Gujar, K.D. Jung, O.S. Joo, Simple chemical preparation of CuS nanowhiskers, *Mater. Sci. Eng. B* 140 (2007) 199–202.

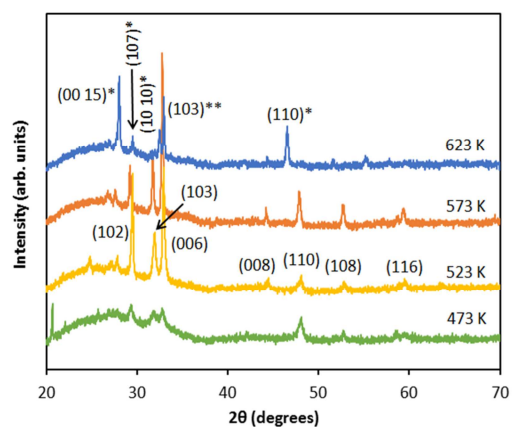
- [11] R. Blachnik, A. Muller, The formation of Cu<sub>2</sub>S from the elements: I. Copper used in form of powders, *Thermochim. Acta* 361 (2000) 31-52.
- [12] K. Tezuka, W.C. Sheets, R. Kurihara, Y. J. Shan, H. Imoto, T. J. Marks, K. R. Poeppelmeier, Synthesis of covellite (CuS) from the elements, *Solid State Sci.*, 9 (2007) 95-99.
- [13] P. Kalyanaraman, N. Vijayashree, A.G. Samuelson, Low temperature synthesis and interconversions of copper sulphides using acetonitrile, India. *J. Chem. Sect. A*, 33A, (1994), 281-283.
- [14] R.S. Mane, C.D. Lokhande, Chemical deposition method for metal chalcogenide thin films, *Mater. Chem. Phys.*, 65, (2000), 1-31.
- [15] M. T. S. Nair, P. K. Nair, Near-ideal solar control characteristics of Cu<sub>x</sub>S thin films, *Semicond. Sci. Technol.*, 4, (1989), 191-199.
- [16] S.V. Bagula, S.D. Chavhanb, Ramphal Sharma, Growth and characterization of Cu<sub>x</sub>S (x=1.0, 1.76, and 2.0) thin films grown by solution growth technique (SGT), *J. Phys. Chem. Solid.*, 68 (2007) 1623–1629.
- [17] L. A. Isac, A Duta, A. Kriza, I. A. Enesca, M. Nanu, The growth of CuS thin films by Spray Pyrolysis, *J. Phys. Conf. Ser.*, 61, (2007), 477–481.
- [18] S. B. Gadgil, R Thangaraj & O. P. Agnihotri, Optical and solar selective properties of chemically sprayed copper sulphide films, *J. Phys. D, Appl. Phys.*, 20, (1987), 112-115.
- [19] Y.B. He, A. Politya, I. O. Sterreichera, D. Pfisterera, R. Gregora, B.K. Meyera, M. Hardt, Phys. B, Hall effect and surface characterization of Cu<sub>2</sub>S and CuS films deposited by RF reactive sputtering, 308–310, (2001), 1069–1073.
- [20] H. S. Randhawa, R. F. Bunshah, D. G. Brock, B. M. Basol and O. M. Stafsudd, Preparation of Cu<sub>x</sub>S thin films by activated reactive evaporation technique, *Sol. Energ. Mater.*, 6, (1982), 445-453.
- [21] J. Asmussen, Electron cyclotron resonance microwave discharges for etching and thin-film deposition, *J. Vac. Sci. Technol.*, A 7 (1989) 883.
- [22] L. Wang, H. S. Reehal, Low temperature growth of p-type crystalline silicon films by ECR plasma CVD, *Thin Solid Film.*, 343-344, (1999), 571-574.
- [23] K. Sasaki, T. Takada, *Jpn J. of Appl. Phys.*, 37, (1998), 402.
- [24] J. Ball, H.S. Reehal, *Thin Solid Film.*, 520 (2012) 2467–2473.
- [25] International Centre for Diffraction Data, 12 Campus Boulevard, Newtown Square, PA 19073-3273 U.S.A
- [26] M T S Nair, L. Guerrero and P. K. Nair, *Semicon. Sci. Technol.*, 13, (1998), 1164-1169.

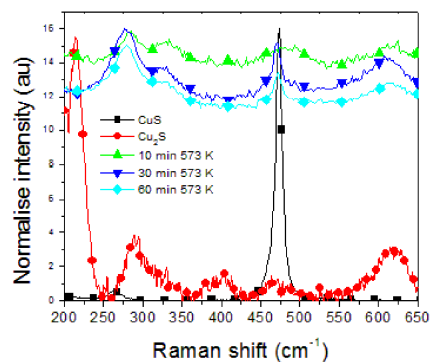
- [27] S.D. Sartale, C.D. Lokhande, *Mater. Chem. Phys.*, 65, (2000), 63–67.
- [28] B. Ren, L. Wang, J. Huang, K. Tang, Y. Yang, L. Wang, *Vac.*, 112 (2015) 70-72.
- [29] M. Xin, K. W. Li, H. Wang, *Appl. Surf. Sci.*, 256 (2009) 1436–1442.
- [30] K-J Wang, G-D Li, J-X Li, Q Wang and J-Sheng Chen, *Cryst Grow. Des.*, 7, (2007), 2265–2267.
- [31] K.M. Gadave, C.D. Lokhande, *Thin Solid Film.*, 229, (1993), 1-4.
- [32] H. Katagiri, K. Jimbo, W. Shwe Maw, K. Oishi, M. Yamazaki, H. Araki, A. Takeuchi *Thin Solid Film.*, 517, (2009), 2455–2460.
- [33] T. P. Dhakal, C–Y. Peng, R. R. Tobias, R. Dasharathy, C. R. Westgate, *Sol. Energ.*, 100, (2014), 23–30.
- [34] X. Liu, Y. Feng, H. Cui, F. Liu, X. Hao, G. Conibeer, D. B. Mitzi, M. Green, *Prog. Photovolt: Res Appl*, 24, (2016), 879–898.

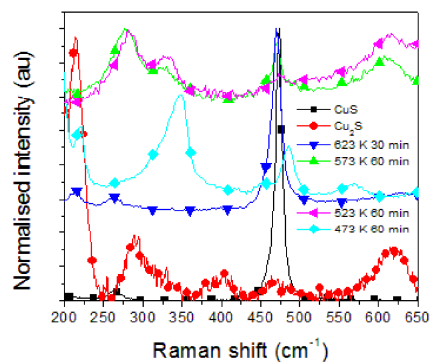


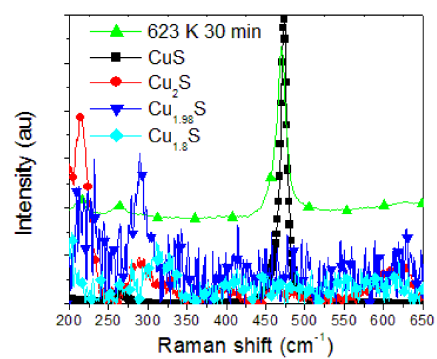


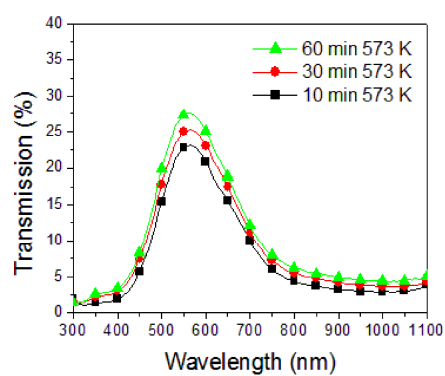


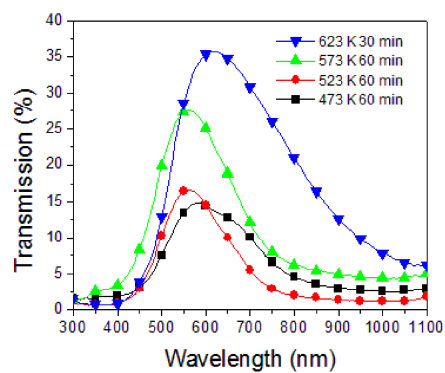


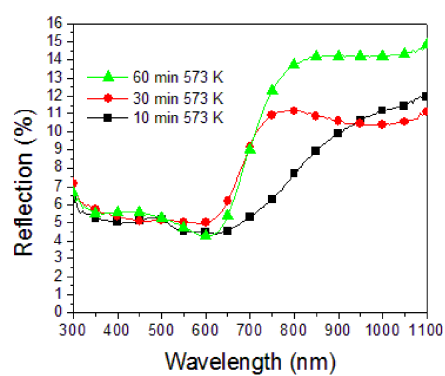


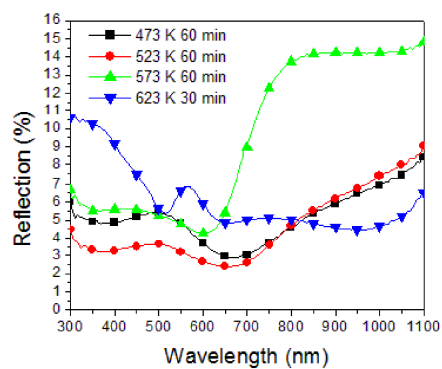


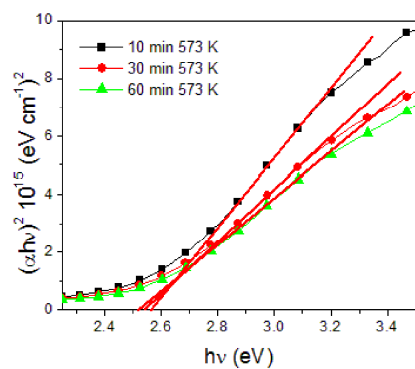


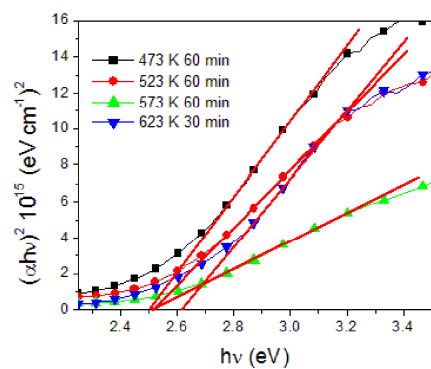


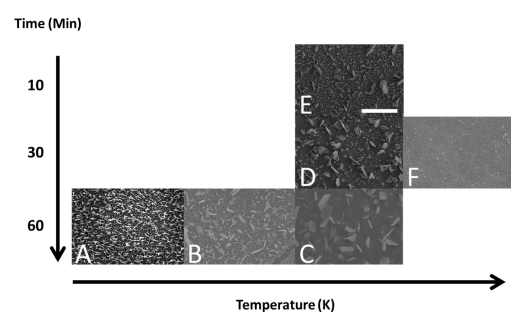












**Highlights**

The synthesis of  $\text{Cu}_x\text{S}$  from Cu layers by low pressure plasma processing

J Ball<sup>a\*</sup>, D W Lane<sup>b</sup> & H S Reehal<sup>a</sup>

<sup>a</sup>School of Engineering, London South Bank University, 103 Borough Road, London SE1 0AA, UK.

<sup>b</sup>Materials Science and Radiation Group, Cranfield Forensic Institute, Cranfield, Defence and Security, Cranfield University, Shrivenham, Swindon, SN6 8LA, UK

- A new method of converting Cu layers to  $\text{Cu}_x\text{S}$  using plasma and  $\text{SF}_6$  gas is presented.
- Trends in film crystallinity/morphology in relation to process time/temperature.
- Sulphurisation is most likely complete within 10 minutes.

# The synthesis of $Cu_xS$ from Cu layers by low pressure plasma processing

Ball, J.

2017-03-04

Attribution-NonCommercial-NoDerivatives 4.0 International

---

Ball J, Lane DW, Reehal HS. (2017) The synthesis of  $Cu_xS$  from Cu layers by low pressure plasma processing, Journal of Alloys and Compounds, Volume 708, June 2017, pp. 1124-1130  
<http://dx.doi.org/10.1016/j.jallcom.2017.03.011>

*Downloaded from CERES Research Repository, Cranfield University*